CHARGE FORMFACTORS AND DENSITIES OF ^{2}D, ^{3}H, ^{3}He, AND ^{4}He NUCLEI

YU.A. BEREZHNOY, V.YU. KORDA[1], A.G. GAKH

V.N. Karazin Kharkiv National University
(4, Svoboda Sq., Kharkiv 61077, Ukraine; e-mail: agakh@mail.ru),

[1]Institute for Electrophysics and Radiation Technology, Nat. Acad. of Sci. of Ukraine
(28, Chernyshevskyi Str., Kharkiv 61002, Ukraine)

UDC 539.17

A new non-relativistic analytical phenomenological model for ^{2}D, ^{3}H, ^{3}He, and ^{4}He nuclei has been developed. The wave function parameters for the ground states of those nuclei have been determined by analyzing the experimentally measured charge formfactors, root-mean-square radii, and binding energies. The obtained wave functions have been used to calculate the charge densities in the nuclei concerned.

1. Introduction

The lightest nuclei attract a certain interest, because exact solutions for a large number of nuclear properties can be obtained in this case, proceeding immediately from a realistic model nucleon-nucleon interaction. Nuclei with a few nucleons enable a rather large number of problems to be studied. Unlike heavy nuclei, the nuclei under consideration are characterized by a large density gradient, and their surface region practically coincides with the nucleus itself. Three-nucleon nuclei enable one to study almost identical systems, which differ from one another only by swapping protons for neutrons and *vice versa*.

For today, great progress has been achieved in constructing the wave functions for light nuclei. For a good many observable quantities, the discrepancies in their values depend substantially on the physical assumptions rather than on the approximations that were used in calculations. Experiments dealing with the electron scattering by nuclei provide a reliable basis for a detailed verification of theoretical calculations of nuclear wave functions – a basis, which is more important than the integral observables themselves (state energies, moments, and others).

To describe the magnitudes of charge and magnetic formfactors, which are measured in experiments on the electron scattering by nuclei, one has to know the wave function of the examined nucleus in its ground state. The wave function can be found in the framework of various methods and approaches, the majority of which are non-relativistic. In non-relativistic approaches, the wave function of a deuteron is obtained as a solution of the Schrödinger equation for interacting nucleons with the use of one of the realistic nucleon-nucleon potentials that describe well all experimental data concerning the nucleon-nucleon scattering. The following approaches are used for three-nucleon nuclei: the solution of the Faddeev system of equations, correlated hyperspherical harmonics, and the variational Monte Carlo method; three-particle forces have also to be taken into consideration.

Nowadays, there is a large enough body of experimental data on electromagnetic formfactors which can be used to determine the most suitable wave functions for light nuclei. Below, we construct the wave functions of the lightest nuclei, proceeding from experimental data on the scattering of charged particles by nuclei, the root-mean-square radii, the quadrupole moments, and the binding energies of those nuclei. In such an approach, there is no necessity to use a model nucleon-nucleon potential.

2. Deuteron Formfactors

The charge, $G_C(q)$, and quadrupole, $G_Q(q)$, formfactors of a deuteron and the structure function $A(q)$ are determined by the following formulas, provided that the contribution of a term proportional to the magnetic formfactor is neglected [1]:

$$G_C(q) = G_E^S(q) \int_0^\infty dr \left[u^2(r) + w^2(q)\right] j_0\left(\frac{qr}{2}\right), \qquad (1)$$

$$G_Q(q) = G_E^S(q) \frac{3}{2\sqrt{2}\eta} \int_0^\infty dr \left[2u(r)w(r) - \frac{w^2(q)}{\sqrt{2}}\right] \times$$
$$\times j_2\left(\frac{qr}{2}\right), \qquad (2)$$

$$A(q) = G_C^2(q) + \frac{8}{9}\eta^2 G_Q^2(q), \ \eta = q^2/4m_d^2, \qquad (3)$$

where m_d is the deuteron mass, and $G_E^S(q)$ is the electric isoscalar formfactor of nucleon, which is traditionally selected in the form $G_E^S(q) = \left[1 + (0.278q)^2)\right]^{-2}$ [2].

Our research aims at determining such phenomenological functions $u(r)$ and $w(r)$, which would enable the experimental data on electromagnetic formfactors and static characteristics of a deuteron to be described well. Let us express the functions $u(r)$ and $w(r)$ in the form

$$u(r) = \frac{N}{\sqrt{4\pi}} \sum_{k=1}^{n_u} C_k \exp(-\alpha_k r), \tag{4}$$

$$w(r) = \frac{N\rho}{\sqrt{4\pi}} \sum_{k=1}^{n_w} D_k \exp(-\beta_k r) \left(1 + \frac{3}{\beta_k r} + \frac{3}{(\beta_k r)^2}\right), \tag{5}$$

where

$$N = \left(\sum_{k,j=1}^{n_u} \frac{C_k C_j}{\alpha_k + \alpha_j} + \rho^2 \sum_{k,j=1}^{n_w} \frac{D_k D_j}{\beta_k + \beta_j} \right)^{-1/2}, \tag{6}$$

α_i, β_i, C_i, D_i, and ρ are the real-valued variable parameters of the model (α_i, β_i, and ρ are positive numbers, whereas C_i and D_i are arbitrary ones). For the parameters α_i and β_i, we suppose that $\alpha_1 = \beta_1 = \alpha$ and $\alpha_i > \alpha_1$, $\beta_i > \beta_1$ ($i \geq 2$), where $\alpha = \sqrt{M\varepsilon}/\hbar = 0.2316$ Fm^{-1}, and M and $\varepsilon = 2.2245$ MeV are the reduced mass and the binding energy of a deuteron, respectively. Formulas (4) and (5) at $n_u = 1$ and $\rho = 0$ coincide with the Yukawa wave function and, at $n_u = 2$ and $\rho = 0$, with the Hultén wave function [3].

Let us substitute the functions $u(r)$ and $w(r)$ in forms (4) and (5), respectively, into formulas (1) and (2). Then, we obtain

$$G_C(q) = G_E^S(q) \left[F_C^{(S)}(q) + F_C^{(D)}(q)\right], \tag{7}$$

$$F_C^{(S)}(2q) = \frac{N^2}{q} \sum_{k,j=1}^{n_u} C_k C_j \arctan\frac{q}{\alpha_k + \alpha_j}, \tag{8}$$

$$F_C^{(D)}(2q) = \frac{N^2\rho^2}{q} \sum_{k,j=1}^{n_w} D_k D_j \arctan\frac{q}{\beta_k + \beta_j} \times$$

$$\times \left\{1 + \frac{3}{2\beta_k^2}\left[q^2 + (\beta_k + \beta_j)^2\right] + \right.$$

$$\left. + \frac{3}{8\beta_k^2\beta_j^2}\left[q^4 - (\beta_k + \beta_j)^4\right]\right\}. \tag{9}$$

$$G_Q(2q) = G_E^S \frac{3}{2\sqrt{2}\eta} \left(\frac{N^2\rho}{4q^3} \sum_{k=1}^{n_u}\sum_{j=1}^{n_w} B_{kj}^{(1)} - \right.$$

$$\left. - \frac{N^2\rho^2}{\sqrt{2}} \sum_{k,j=1}^{n_w} B_{kj}^{(2)} \right), \tag{10}$$

$$B_{kj}^{(1)}(2q) = \frac{C_k D_j}{\beta_j^2} \left\{ 3q\alpha_k^2\beta_j + \left[3q^4 + q^2(6\alpha_k^2 - 2\beta_j^2) + \right.\right.$$

$$\left.\left. + 3(\alpha_k^2 - \beta_j^2)^2\right] \arctan\frac{q}{\alpha_k + \beta_j} \right\}, \tag{11}$$

$$B_{kj}^{(2)}(2q) = \frac{3}{16} D_k D_j \left\{ \frac{3\beta_j^3 - \beta_k^3}{q^2\beta_k\beta_j} + \frac{1}{q^3\beta_k^2\beta_j^2} \left[-q^6 + \right.\right.$$

$$+ q^4(-3\beta_k^2 + \beta_j^2) + q^2\left(-3\beta_k^4 + \frac{2}{3}\beta_k^2\beta_j^2 + 5\beta_j^4\right) -$$

$$\left.\left. - (\beta_k^2 - 3\beta_j^2)(\beta_k^2 - \beta_j^2)^2\right] \arctan\frac{q}{\beta_k + \beta_j} \right\}. \tag{12}$$

In order to simplify formulas (8), (9), (11), and (12), the argument of the corresponding functions was taken to be $2q$.

The optimum values of model parameters were found making use of the genetic algorithm. The function to be minimized contained a standard quantity χ^2 for experimental points of $G_C(q)$ and $A(q)$, as well as the following information concerning the experimentally observable static characteristics of a deuteron: the root-mean-square radius taking the proton dimension into account, $\langle r^2\rangle_d^{1/2} = 2.094$ Fm; the quadrupole moment of a deuteron $Q = 0.2859$ Fm^2; and its binding energy $\varepsilon = 2.2245$ MeV. An additional condition consisted in the choice of a minimally possible number of terms in sums (4) and (5) and the minimal total number of parameters, which provide agreement with experimental data in the range $q < 7$ Fm^{-1}, because now we have complete information on formfactors just in this range. It can be attained by applying the following relations:

$$\sum_k C_k = 0, \ \sum_k C_k\alpha_k = 0, \ \sum_k D_k = 0, \ \sum_k \frac{D_k}{\beta_k^2} = 0. \tag{13}$$

If these relations are satisfied, the wave functions behave as follows as $r \to 0$: $u(r) \sim r^2$ and $w(r) \sim r^3$.

Our calculations showed that, until the nucleon formfactor remains a separate multiplier in formulas (1)–(3), it is impossible to put in agreement the calculated and experimentally measured values for

electromagnetic formfactors and static characteristics of a deuteron. This circumstance is also confirmed by the results of researches cited in review [4]. Therefore, we applied another procedure: the multiplier $G_E^S(q)$ was put equal to unity in formulas (7)–(10). The physical meaning of this procedure consists in that the information concerning the nucleon structure is contained in parameters of the radial functions $u(r)$ and $w(r)$.

The results of corresponding calculations are depicted in Fig. 1 and are quoted in Tables 1 and 2. Table 1 also contains notations used in Fig. 1 for experimental points. Table 2 includes the parameters of the functions $u(r)$ and $w(r)$, as well as the magnitudes of static characteristics found for a deuteron. Our model contains 5 parameters. In Fig. 1, charge formfactor (1) and structure function (3), both constructed for the deuteron radial functions (4) and (5) with parameters taken from Table 2, are plotted. Some experimental points (stars and squares) are not visible in Fig. 1, because the density of their arrangement in the range of small q is very high. From this figure, one can see that the calculated charge formfactor agrees with experimental data within the whole q-range, and its minimum is located at $q \approx 4.5$ Fm^{-1}, which coincides with the results of the model-free analysis [5]. The results of calculations of the structure function by formula (3)

T a b l e 1. Experimental data for quantities $G_C(q)$ and $A(q)$, and notations for experimental points in Fig. 1

Symbol	Point number	Year	Source
	Experimental data for $G_c(q)$		
△	3	1966	[6]
◇	9	1994	[7]
▽	4	2000	[5]
	Experimental data for $A(q)$		
★	6	1962	[8]
•	5	1965	[9]
□	3	1966	[10]
○	10	1971	[11]
◁	16	1981	[12]
▷	11	1999	[13]

T a b l e 2. Parameters of the calculated wave function of a deuteron and the calculated static characteristics

k	α_k (Fm^{-1})	C_k	β_k (Fm^{-1})	D_k
1	0.2316	1.0	0.2316	1.0
2	1.82007	–136.26749	1.07145	287.15485
3	1.83181	135.26749	1.03542	–288.15485
$Q = 0.2859$ Fm^2		$\langle r^2\rangle^{1/2} = 2.108$ Fm		$\rho = 0.033$

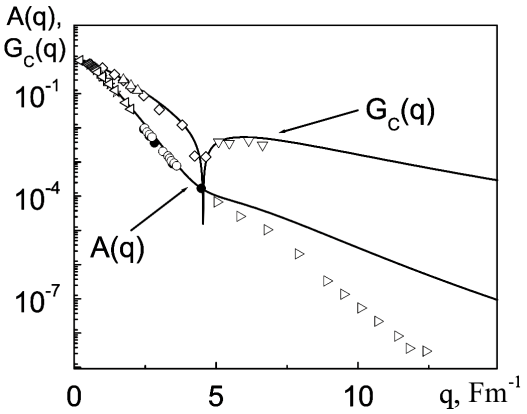

Fig. 1. Dependences of the charge formfactor $G_C(q)$ and the structure function $A(q)$ of a deuteron on the transferred momentum. Notations for experimental points are given in Table 1

agree with experimental data in the range $q \approx 5$ Fm^{-1}. At the same time, in the range of large transferred momenta, the calculated values of the structure function $A(q)$ do not agree with experiment (Fig. 1), which is a characteristic feature of all modern non-relativistic phenomenological models [4]. The discrepancy between experimental data and the results of calculations carried out in the framework of non-relativistic theories can be eliminated only if meson exchange currents, relativistic effects, and quark degrees of freedom are additionally made allowance for.

3. Formfactors of ^{3}H and ^{3}He nuclei

If the term proportional to the magnetic formfactor is neglected, the charge formfactor $G_C(q)$ of ^{3}H and ^{3}He nuclei looks like [14]

$$G_C(q) = \frac{1}{3}[G_1(q) + G_2(q) + G_3(q)], \tag{14}$$

where the nuclear structure factors are

$$G_{1,2}(q) = \int d^3\rho d^3r \exp\left(i\frac{\mathbf{q}}{3}\mathbf{w} \pm i\frac{\mathbf{q}}{2}\mathbf{s}\right)|\Psi_0(\boldsymbol{\rho},\mathbf{r})|^2,$$
$$G_3(q) = \int d^3\rho d^3r \exp\left(-i\frac{2\mathbf{q}}{3}\mathbf{w}\right)|\Psi_0(\boldsymbol{\rho},\mathbf{r})|^2. \tag{15}$$

Here, $\Psi_0(\boldsymbol{\rho},\mathbf{r})$ is the wave function of a three-nucleon nucleus in the ground state, $\boldsymbol{\rho}$ and $\mathbf{r}$ are the Jacobi coordinates, $\mathbf{w}$ and $\mathbf{s}$ are the projections of vectors $\boldsymbol{\rho}$ and $\mathbf{r}$, respectively, onto the plane that is perpendicular to the direction of the beam of bombarding nuclei (axis z).

The wave functions $\Psi_0(\boldsymbol{\rho},\mathbf{r})$ should be so constructed that they describe well experimental data on the charge

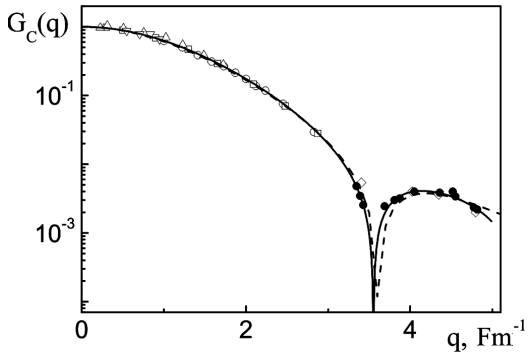

Fig. 2. Dependences of the charge formfactor $G_C(q)$ for ^{3}H nucleus on the transferred momentum: the results of our calculations (solid curve) and the best SOG parametrization [6] (dashed curve). Notations for experimental points are given in Table 3

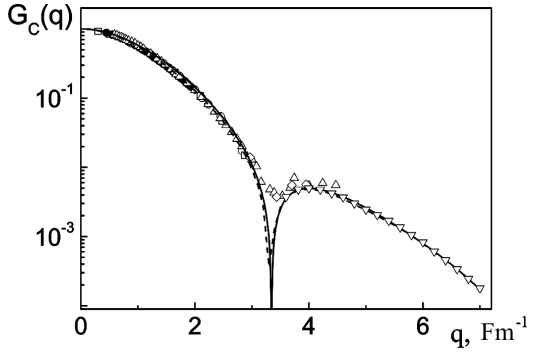

Fig. 3. Dependences of the charge formfactor $G_C(q)$ for ^{3}He nucleus on the transferred momentum: the results of our calculations (solid curve) and the best SOG parametrization [6] (dashed curve). Notations for experimental points are given in Table 5

formfactor and the static characteristics of ^{3}H and ^{3}He nuclei. We seek the wave function $\Psi_0(\boldsymbol{\rho}, \mathbf{r})$ in the form

$$\Psi_0(\boldsymbol{\rho}, \mathbf{r}) = \psi_0(\boldsymbol{\rho})\varphi_0(\mathbf{r}), \tag{16}$$

where

$$\varphi_0(r) = \frac{N_1}{\sqrt{4\pi}} \sum_{k=1}^{n_1} C_k \frac{\exp(-\alpha_k r)}{r}, \tag{17}$$

$$\psi_0(\rho) = \frac{N_2}{\sqrt{4\pi}} \sum_{k=1}^{n_2} D_k \frac{\exp(-\beta_k \rho)}{\rho}, \tag{18}$$

$$N_1 = \left(\sum_{k,j=1}^{n_1} \frac{C_k C_j}{\alpha_k + \alpha_j} \right)^{-1/2},$$

$$N_2 = \left(\sum_{k,j=1}^{n_2} \frac{D_k D_j}{\beta_k + \beta_j} \right)^{-1/2}, \tag{19}$$

α_i, β_i, C_i, and D_i are the real-valued parameters of the model which are to be varied (α_i and β_i are positive numbers, whereas C_i and D_i can be of either sign). To describe experimental values of the binding energy of the nuclei under consideration, the model parameters have to satisfy the conditions

$$\frac{3}{4}\beta_1^2 + \alpha_1^2 = \frac{m\varepsilon}{h^2}, \quad \alpha_i > \alpha_1, \quad \beta_i > \beta_1, \quad i \geq 2, \tag{20}$$

where m is the nucleon mass, and ε is the binding energy of the three-nucleon nucleus ($\varepsilon = \varepsilon_t = 8.479$ MeV for ^{3}H nucleus, and $\varepsilon = \varepsilon_h = 7.719$ MeV for ^{3}He one). For the wave function to be regular at zero argument value, the first and third relations in formulas (13) are to be obeyed.

By substituting expressions (16)–(19) into formulas (14) and (15), we obtain

$$G_C(q) = \frac{1}{3}\left\{ 2G\left(\frac{q}{3}\right) S\left(\frac{q}{2}\right) + G\left(\frac{2q}{3}\right) \right\}, \tag{21}$$

$$S(q) = \frac{N_1^2}{q} \sum_{k,j=1}^{n_1} C_k C_j \arctan\left(\frac{q}{\alpha_k + \alpha_j} \right), \tag{22}$$

$$G(q) = \frac{N_2^2}{q} \sum_{k,j=1}^{n_2} D_k D_j \arctan\left(\frac{q}{\beta_k + \beta_j} \right). \tag{23}$$

The optimum values of model parameters were found making use of the genetic algorithm. The function to be minimized contained a standard quantity χ^2 for experimental points for the charge formfactor $G_C(q)$ and the root-mean-square radius of a three-nucleon nucleus, taking the proton dimension into account: $\langle r^2 \rangle_t^{1/2} = 1.700$ Fm and $\langle r^2 \rangle_h^{1/2} = 1.877$ Fm. An extra condition consisted in the choice of a minimal number of terms in sums (17) and (18) and the minimal total number of fitting parameters, which would provide agreement with experimental data.

The results of corresponding calculations are depicted in Figs. 2 and 3, and are quoted in Tables 3 to 6. In Figs. 2 and 3, the solid curves correspond to the charge formfactor $G_C(q)$ for nuclei ^{3}H and ^{3}He, respectively, constructed for wave function (16)–(19) with the parameters taken from Tables 3 and 5. The dashed curves illustrate the best SOG (sum-of-Gaussians) parametrization [7] for the formfactor $G_C(q)$; it is included for the sake of comparison with the results obtained. It is evident from the figures that the

charge formfactor calculated in the framework of our model agrees with experimental data within the range of transferred momentum $q^2 \leq 25$ Fm^{-2}. Table 3 contains notations used in Fig. 2 for experimental points, and Table 5 those used in Fig. 3. In Figs. 2 and 3, some experimental points for the formfactor $G_C(q)$ are not visible, owing to their high density in the range of small q. The parameters of the wave functions $\psi_0(\boldsymbol{\rho})$ and $\varphi_0(\mathbf{r})$ and the values of root-mean-square radius and binding energy for nuclei ^{3}H and ^{3}He are quoted in Tables 4 and 6, respectively. Our model contains 8 fitting parameters. The SOG parametrization mentioned above [7] includes 20 parameters for ^{3}H nucleus and 23 parameters for ^{3}He one.

4. α-particle Formfactor

If the term proportional to the magnetic formfactor is neglected, the charge formfactor $G_C(q)$ of ^{4}He nucleus looks like [14]

$$G_C(q) = \frac{1}{4}[G_1(q) + G_2(q) + G_3(q) + G_4(q)], \qquad (24)$$

where the structure factors of the nucleus are

$$G_{1,2}(q) = \int d^3\xi d^3\eta \exp\left(i\frac{\mathbf{q}}{2}\mathbf{w} \pm i\frac{\mathbf{q}}{2}\mathbf{s}\right)|\Psi_0(\boldsymbol{\xi},\boldsymbol{\zeta},\boldsymbol{\eta})|^2,$$
$$G_{3,4}(q) = \int d^3\zeta d^3\eta \exp\left(i\frac{\mathbf{q}}{2}\mathbf{v} \pm i\frac{\mathbf{q}}{2}\mathbf{s}\right)|\Psi_0(\boldsymbol{\xi},\boldsymbol{\zeta},\boldsymbol{\eta})|^2. \qquad (25)$$

Here, $\Psi_0(\boldsymbol{\xi}, \boldsymbol{\zeta}, \boldsymbol{\eta})$ is the wave function of ^{4}He nucleus in the ground state; $\boldsymbol{\xi}$, $\boldsymbol{\zeta}$, and $\boldsymbol{\eta}$ are relative coordinates associated with the coordinates of nucleons in the nucleus by the relations $\boldsymbol{\xi} = \mathbf{r}_2 - \mathbf{r}_1$, $\boldsymbol{\zeta} = \mathbf{r}_4 - \mathbf{r}_3$, and $\boldsymbol{\eta} = (\mathbf{r}_3 + \mathbf{r}_4 - \mathbf{r}_1 - \mathbf{r}_2)/2$; and $\mathbf{w}$, $\mathbf{v}$, and $\mathbf{s}$ are the projections of vectors $\boldsymbol{\xi}$, $\boldsymbol{\zeta}$, and $\boldsymbol{\eta}$, respectively, onto the plane that is perpendicular to the direction of the beam of bombarding nuclei (axis z).

We seek the wave function $\Psi_0(\boldsymbol{\xi}, \boldsymbol{\zeta}, \boldsymbol{\eta})$ in the form

$$\Psi_0(\boldsymbol{\xi},\boldsymbol{\zeta},\boldsymbol{\eta}) = \boldsymbol{\varphi_0}(\boldsymbol{\xi})\boldsymbol{\varphi_0}(\boldsymbol{\zeta})\boldsymbol{\psi_0}(\boldsymbol{\eta}), \qquad (26)$$

where the functions $\varphi_0(\boldsymbol{\xi})$ and $\varphi_0(\boldsymbol{\zeta})$ are selected in form (17), and the function $\psi_0(\boldsymbol{\eta})$ in form (18). To describe the experimental value of binding energy for α-particle, the model parameters must satisfy the conditions

$$\frac{\beta_1^2}{2} + 2\alpha_1^2 = \frac{m\varepsilon_\alpha}{h^2}, \quad \alpha_i > \alpha_1, \quad \beta_i > \beta_1, \quad i \geq 2, \qquad (27)$$

where the binding energy of ^{4}He nucleus is $\varepsilon_\alpha = 28.3$ MeV. For the wave function to be regular at zero argument value, the first and third relations in formulas (13) are to be obeyed.

By substituting expressions (26), (17), and (18) into formulas (24) and (25), we obtain

$$G_C(q) = G\left(\frac{q}{2}\right)S\left(\frac{q}{2}\right). \qquad (28)$$

The optimum values of model parameters were found making use of the genetic algorithm. The function to be minimized contained the standard quantity χ^2 for experimental points for the charge formfactor $G_C(q)$ and

T a b l e 3. Experimental data for the charge formfactor $G_C(q)$ of ^{3}H nucleus and notations for experimental points in Fig. 2

Symbol	Point number	Year	Source
◯	11	1965	[15]
▽	4	1982	[16]
△	8	1984	[17]
•	12	1985	[18]
□	8	1987	[19]
◇	4	1994	[7]

T a b l e 4. Parameters of the calculated wave function and the calculated root-mean-square radius and binding energy for ^{3}H nucleus

k	α_k (Fm^{-1})	C_k	β_k (Fm^{-1})	D_k
1	0.276440	1.0	0.414360	1.0
2	0.565724	698.825	0.886278	319.495
3	0.561797	–699.825	1.64959	378.156
4	–	–	1.25411	-698.651
$\langle r^2\rangle_t^{1/2} = 1.700$ Fm			$\varepsilon_t = 8.4786$ MeV	

T a b l e 5. Experimental data for the charge formfactor $G_C(q)$ of ^{3}He nucleus and notations for experimental points in Fig. 3

Symbol	Point number	Year	Source
◯	11	1965	[15]
▽	4	1972	[20]
△	42	1977	[21]
▷	18	1978	[22]
•	24	1985	[23]
□	8	1987	[19]

T a b l e 6. Parameters of the calculated wave function and the calculated root-mean-square radius and binding energy for ^{3}He nucleus

k	α_k (Fm^{-1})	C_k	β_k (Fm^{-1})	D_k
1	0.173265	1.0	0.456204	1.0
2	0.832802	608.783	0.826155	–489.795
3	2.780747	443.930	0.459225	377.686
3	1.418167	–1053.713	2.730292	111.109
$\langle r^2\rangle_h^{1/2} = 1.877$ Fm			$\varepsilon_h = 7.7194$ MeV	

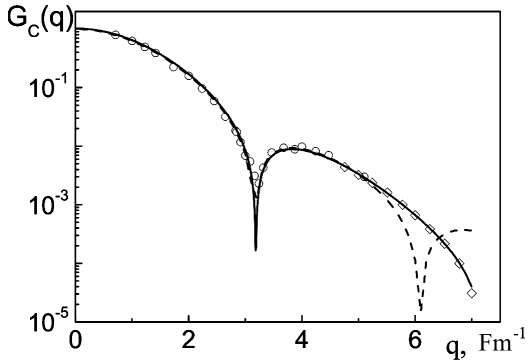

Fig. 4. Dependences of the charge formfactor $G_C(q)$ for ^{4}He nucleus on the transferred momentum: the results of our calculations (solid curve) and the results of calculations in the framework of the model-free approach [27] (dashed curve). Notations for experimental points are given in Table 7

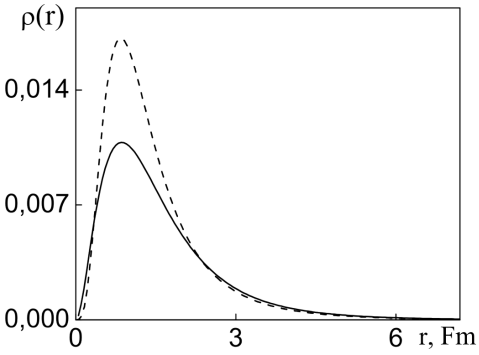

Fig. 5. Distributions of the substance density $\rho(r)$ in a deuteron: the results of our calculations for non-point nucleons (solid curve) and the results of calculations in the framework of the McGee model in the point-nucleon approximation [26] (dashed curve)

the root-mean-square radius of ^{4}He nucleus, taking the proton dimension into account: $\langle r^2\rangle_\alpha^{1/2} = 1.676$ Fm.

The results of corresponding calculations are depicted in Fig. 4 and are quoted in Tables 7 and 8. In Fig. 4, the solid curve corresponds to the charge formfactor $G_C(q)$ for ^{4}He nucleus, constructed for wave function (26) with the parameters quoted in Table 8. The dashed curve corresponds to the results of calculations in the framework of the model-free approach [27]. It is evident from the figure that the charge formfactor calculated by us agrees with experimental data within the whole measurement range of transferred momentum q ($q < 7$ Fm^{-1}). Table 7 contains the values for the parameters of the wave functions $\varphi_0(\xi)$, $\varphi_0(\zeta)$, and $\psi_0(\eta)$, and the calculated values for the root-mean-square radius and the binding energy of ^{4}He nucleus. Our model contains 10 fitting parameters. The parametrization used in work [27] includes 5 parameters.

5. Charge Density Distribution

The one-particle density distribution in a deuteron can be obtained by means of the radial wave functions $u(r)$ and $w(r)$ found above:

$$\rho(r) = \frac{1}{r^2}\big(u(r)^2 + w(r)^2\big). \tag{29}$$

The results of corresponding calculations, when the functions $u(r)$ and $w(r)$ are taken in forms (4) and (5), respectively, with the parameters taken from Table 2, are depicted in Fig. 5. The discrepancy between the curves in this figure is connected with the fact that we considered nucleons as extended particles, whereas they were assumed to be point ones in work [26].

The distribution of charge density in ^{3}He and ^{4}He nuclei is determined by the Fourier transformation of the charge formfactor $G_C(q)$:

$$\rho(r) = \frac{Ze}{(2\pi)^3}\int G_C(\mathbf{q})e^{-i\mathbf{qr}}d\mathbf{q}, \tag{30}$$

where Ze is the nucleus charge.

The results of calculations of the charge density for helium nuclei are exhibited in Fig. 6. The character of the charge density distribution in ^{3}H nucleus is similar to that in ^{3}He nucleus and includes no additional information. The one-particle charge densities in ^{3}He and ^{4}He nuclei presented in Fig. 6 are characterized by a maximum in the central region of a nucleus, which testifies to a high probability for nucleons to be in this

T a b l e 7. Experimental data for the charge formfactor $G_C(q)$ of ^{4}He nucleus and notations for experimental points in Fig. 4

Symbol	Point number	Year	Source
○	23	1967	[24]
◇	10	1998	[25]

T a b l e 8. Parameters of the calculated wave function and the calculated root-mean-square radius and binding energy for ^{4}He nucleus

k	α_k (Fm^{-1})	C_k	β_k (Fm^{-1})	D_k
1	0.54835	1.0	0.40590	1.0
2	9.16145	65.326	0.62132	–630.103
3	1.16801	227.039	2.18073	–316.653
3	1.87860	–293.365	1.00426	945.756
$\langle r^2\rangle_\alpha^{1/2} = 1.676$ Fm			$\varepsilon_\alpha = 28.3$ MeV	

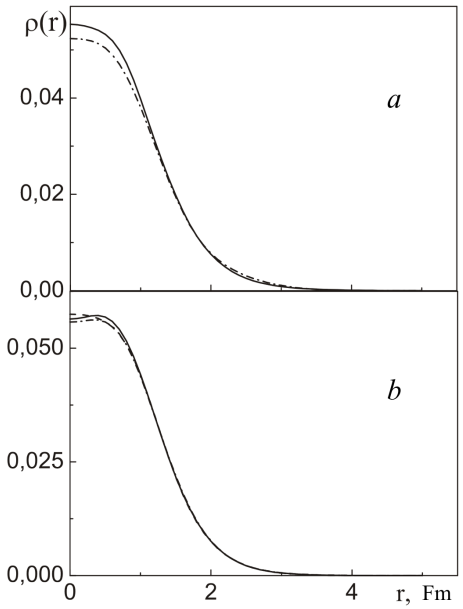

Fig. 6. Distributions of charge density $\rho(r)$ in ^{3}He (a) and ^{4}He (b) nuclei: the results of our calculations for non-point nucleons (solid curve), the results of calculations in the framework of model [27] in the point-nucleon approximation (dashed curve), and the distribution of charge density calculated in work [28] (dash-dotted curve)

region. Note that, unlike the case of helium nuclei, the probability for nucleons to be in the central part of a deuteron is close to zero, and the most probable distance between the nucleon and the deuteron center amounts to $r_{\max} = 0.85$ Fm.

6. Conclusions

The differential cross-sections of elastic electron scattering by nuclei differ from the Rutherford ones, because the electric charge of a nucleus is non-point. The discrepancy between those cross-sections is described by the nuclear charge formfactor $G_C(q)$ which contains information on the spatial distribution of electric charge in the nucleus and, as a consequence, information on the root-mean-square nuclear radius and the nuclear surface smearing. Hence, the experimental determination of nuclear formfactors is important for getting the information on the nuclear structure, which is necessary, in its turn, for the construction of correct nuclear models and the description of the interaction of particles with nuclei, without engaging additional fitting parameters.

The results of numerous experiments testify that the nuclear formfactors are oscillating functions of the transferred momentum (the scattering angle), and that they quickly decrease as q grows (Figs. 1–4). Therefore, the measurement of formfactors for large enough q (large scattering angles) is a complicated experimental task, because the cross-sections are small in this range. However, knowing the formfactor magnitudes for large q is important, because just this range of transferred momenta contains the information on the behavior of the electric charge density distribution in the central part of a nucleus.

The one-particle charge density distribution in a nucleus is a Fourier transform of the charge formfactor $G_C(q)$. The charge density in three-nucleon and heavier nuclei is characterized by a peak in the central part of the nucleus; then it smoothly vanishes. At the same time, for a deuteron, the density is close to zero at the center of the nucleus and has a maximum at $r_{\max} = 0.85$ Fm. Such a behavior of the charge density in a deuteron is associated with the fact that both the neutron and the proton are mainly located at some distance from the deuteron center of mass.

1. A.I. Akhiezer, A.G. Sitenko, and V.K. Tartakovskii, *Nuclear Electrodynamics* (Springer, Berlin, 1994).
2. T. Ericson and W. Weise, *Pions and Nuclei* (Clarendon Press, Oxford, 1988).
3. L. Hulthén and S. Skavlem, Phys. Rev. **87**, 297 (1952).
4. R. Gilman and F. Gross, J. Phys. G **28**, R37 (2002).
5. D. Abbott, A. Ahmidouch, H. Anklin et al., Eur. Phys. J. A **7**, 421 (2000).
6. D. Benaksas, D. Drickey, and D. Frerejacque, Phys.Rev. **148**, 1327 (1966).
7. A. Amroun, V. Breton, J.-M. Cavedon *et al.*, Nucl. Phys. A **579**, 596 (1994).
8. D.J. Drickey and L.N. Hand, Phys. Rev. Lett. **9**, 521 (1962).
9. C.D. Buchanan and M.R. Yearian, Phys. Rev. Lett. **15**, 303 (1965).
10. B. Grossetete, D. Drickey, and P. Lehmann, Phys. Rev. **141**, 1425 (1966).
11. S. Galster, H. Klein, and J. Moritz, Nucl. Phys. B **32**, 221 (1971).
12. G.G. Simon, Ch. Schmitt, and V.H. Walther, Nucl. Phys. A **364**, 285 (1981).
13. L.C. Alexa, B.D. Anderson, K.A. Aniol *et al.*, Phys. Rev. Lett. **82**, 1374 (1999).
14. M.L. Goldberger and K.M. Watson, *Collision Theory* (Wiley, New York, 1964).
15. H. Collard, R. Hofstadter, E.B. Huges, A. Johansson, M.R. Yearian, R.B. Dan, and R.T. Wagner, Phys. Rev. **138**, B57 (1965).
16. D.H. Beck, J. Asai, and D.M. Skopik, Phys. Rev. C **25**, 1152 (1982).
17. D.H. Beck, S.B. Kowalski, M.E. Schulze et. al., Phys. Rev. C **30**, 1403 (1984).

18. F.-P. Juster, S. Auffret, J.-M. Cavedon *et al.*, Phys. Rev. Lett. **55**, 2261 (1985).

19. D. Beck, A. Bernstein, I. Blomqvist *et al.*, Phys. Rev. Lett. **59**, 1537 (1987).

20. M. Bernheim, D. Blum, W. McGill *et al.*, Lett. Nuovo Cimento **5**, 431 (1972).

21. J.S. McCarthy, I. Sick, and R.R. Whitney, Phys. Rev. C **15**, 1396 (1977).

22. R.G. Arnold, B.T. Chertok, S. Rock *et al.*, Phys. Rev. Lett. **40**, 1429 (1978).

23. C.R. Ottermann, G. Kobschall, K. Maurer *et al.*, Nucl. Phys. A **436**, 688 (1985).

24. R.F. Frosch, J.S. McCarthy, R.E. Rand, and M.R. Yearian, Phys. Rev. **160**, 874 (1967).

25. J. Carlson and R. Schiavilla, Rev. Mod. Phys. **70**, 743 (1998).

26. I.J. McGee, Phys. Rev. **151**, 772 (1966).

27. V.V. Burov, D.N. Kadrev, V.K. Lukyanov, and Yu.S. Pol', Yad. Fiz. **61**, 595 (1998).

28. H. De Vries, C.W. De Jager, and C. De Vries, At. Data Nucl. Data Tables **36**, 495 (1987).

Received 17.09.08.
Translated from Ukrainian by O.I. Voitenko

ЗАРЯДОВІ ФОРМФАКТОРИ ТА ГУСТИНИ ЯДЕР ^{2}D, ^{3}H, ^{3}He і ^{4}He

Ю.А. Бережной, В.Ю. Корда, А.Г. Гах

Р е з ю м е

Розроблено нову нерелятивістську аналітичну феноменологічну модель ядер ^{2}D, ^{3}H, ^{3}He, ^{4}He. Параметри хвильових функцій цих ядер в основному стані визначено з аналізу експериментально виміряних зарядових формфакторів, середньоквадратичних радіусів та енергій зв'язку. Знайдені хвильові функції застосовано для розрахунків зарядових густин ядер, що розглядаються.